Title
Z-dependence of kaonic atom x-ray intensities

Authors
Godfrey, Gary L.
Wiegand, Clyde E.

Publication Date
1974-07-09

Submitted to Physical Review Letters

LBL-3080
Preprint c.1

Z-DEPENDENCE OF KAONIC ATOM X-RAY INTENSITIES

Gary L. Godfrey and Clyde E. Wiegand

August 1974

Prepared for the U. S. Atomic Energy Commission
under Contract W-7405-ENG-48

LBL-3080

Z-DEPENDENCE OF KAONIC ATOM X-RAY INTENSITIES*

Gary L. Godfrey and Clyde E. Wiegand

Lawrence Berkeley Laboratory
University of California
Berkeley, California 94720

August 1974

Abstract

Mesonic x-ray intensities have a striking dependence on Z. We postulate that different atomic electron configurations cause the mesons to arrive at principal quantum number $n = 30$ (for kaons) with angular momentum distributions that are Z-dependent. Measurements on H_2O and CH show greatly reduced x-ray intensities apparently due to the presence of the hydrogen bonds. No evidence was found for trapping in metastable orbits. The experiment added new data to the Z-dependence of intensities.

Analytic Subject
Index 15

As an explanation for the Z-dependence of kaonic x-ray intensities, we claim that the mesons cascade into orbits of large principal quantum number with angular momentum distributions that depend on the electron configuration or size of the atoms.

We report on a search for metastable mesonic orbits and also add considerable data to our former results.[1] Since compiling the published data we made measurements of kaonic x-ray intensities on many elements that were not previously tried. The experiment was done at the Bevatron with the apparatus described in Ref. 1.

Consider the x-ray intensities of a certain transition in kaonic atoms, for example, $n = 6 \rightarrow 5$, as a function of Z. The curve was expected to rise from almost zero for light elements to a broad maximum and fall to zero for medium-Z elements.[2] For a given transition Auger processes dominate over radiation at low Z whereas for higher Z, mesons encounter nuclear matter and disappear in strong reactions. We found approximately the expected range over Z but the curves have peaks and valleys that are believed to have their origin in atomic effects.

In Fig. 1 we present the new $\Delta n = -1$ points by plotting them as open squares in combination with the earlier data of intensities versus Z. Measurements were repeated on several of the targets and we have plotted both the old and the new points except for rare-earth oxides which were replaced by metallic targets. The error bars are those that correspond to statistics only and do not allow for possible error in the absolute calibration which should apply equally to all the ordinate scales.

We observed that the maxima occurred near the Z of completed atomic shells. We were also cognizant of the fact that the "largest" atoms are those with one electron added to the closed shells and that our intensity curves resemble the plot of atomic size versus Z. Condo [3] also recognized this correlation of intensities to interatomic spacing.

On the other hand, the valleys in the intensity versus Z curves may represent departures from an average of about 0.5 x rays per kaon. A significant minimum occurred around the transition elements, Z = 23, 24, and 25. Probably outer-shell electrons played an important role in the eventual distribution of angular momentum. Kaons that initially fell into angular momentum distributions weighted toward maximum ℓ yielded high x-ray intensities at low-n transitions compared to the situation where kaons were distributed toward lower initial ℓ-states. Mesons that arrived at orbits of maximum ℓ ($\ell = n - 1$) were trapped in these circular orbits for the duration of their cascade. On the contrary, kaons found in less-than-maximum-ℓ states can reach angular momentum states where ℓ is sufficiently low for strong nuclear absorption even though n is large. This happens because, for given n, the overlap of the kaonic wave function with conventional distributions of nuclear matter greatly increases as ℓ decreases.

To substantiate some of these ideas we made intensity calculations via a cascade program. The cascade calculations contained electric dipole radiation rates and Auger transition rates down to 100 eV using Ferrell's [4] formula with the assumption of immediate refilling of vacated states. Calculations included the Fried and Martin[5] factor for nuclear motion. Nuclear absorption was derived from a simple overlap of the atomic kaon and nuclear Saxon-Woods density distribution. We list the equations used to facilitate comparison with other results.

$$\Gamma = W/\hbar \int \rho(r)\, R^2_{n,\ell}\, r^2\, dr, \quad \sec^{-1}$$

$$W = 4\pi\hbar^2 (1/\mu_K)(1 + m_K/m_N)\ \mathrm{Im}\ a_K, \quad \mathrm{MeV}\ F^3$$

$$\rho(r) = \rho(0)\left\{1 + \exp\left[(r - C)\ 4\ln 3/t\right]\right\}^{-1}, \quad F^{-3}$$

$$A = 4\pi \int \rho(r)\, r^2\, dr = \text{mass number}$$

$R_{n,\ell}$ = kaon radial wave function, $F^{-3/2}$

$\mathrm{Im}\ a_K = 0.83$ F = effective K^--N scattering length[6]

μ_K = kaon reduced mass; m_K = kaon mass; m_N = nucleon mass

$C = 1.07\ A^{1/3}$ F; $t = 2.42$ F.

Initial kaon distributions proportional to $2\ell + 1$ at $n = 30$ were used to calculate the absolute intensities. For ^{32}S the $2\ell + 1$ distribution extended to $\ell_{max} = 29$ whereas for ^{55}Mn the distribution was terminated at $\ell_{max} = 18$. (All higher ℓ were considered absent.) ℓ_{max} could be varied by ± 2 and still give satisfactory agreement. Results on several elements are listed in Table I.

The ultimate fate of kaons captured into the Coulomb field of nuclei has been assumed to be annihilation in strong interactions with nucleons in which a hyperon and usually a pion were produced. The time to cascade from capture at large n to low-lying orbits is so much shorter than the kaon lifetime that natural K^- decay is not observed. An exception was K^- in liquid He where about 2% of the kaons were seen to decay.[(7)] However, the idea has been entertained by Condo and by Russell[(8)] that perhaps negative mesons in orbits near maximum angular momentum could become trapped in high n-states for time intervals comparable to those for radiative transitions. Trapping in metastable orbits could result from the suppression of Auger processes. If kaons were delayed in their cascade schedule, we could expect some of them to decay. Accordingly we set up a system to test this idea concurrently with the recording of x rays. A scintillation counter telescope similar to the one described in Ref.1 (for use in beam calibration) was added to the circuitry to look for kaon decays, $K^- \rightarrow \mu^- + \nu$. We found no evidence for kaon decay in any of the targets. The upper limit for the number of decays amounted to about 5 % of the stopped kaons. Attention was focussed on targets of Ar, As, and Se (maximal x-ray intensity) and Mn (minimal intensity). There was no significant difference in the results. If decays had occurred in metastable orbits, we would have expected to observe more decays in Mn than in the other elements. Apparently trapping in metastable states was not a factor in the Z-dependence.

Another ramification of our results was pointed out to us by G. Backenstoss in connection with an experiment on muonic x-ray intensities of elements from S to Mo.[9] Let I_α be the intensity of $2p \rightarrow 1s$ transitions and I_β, I_γ,... intensities of transitions from n = 2, 3, ... to n = 1. It was observed that plots of I_β / I_α versus Z and $(I_\beta + I_\gamma \ldots)/I_\alpha$ versus Z showed minima around Z = 19 and rising steeply to maxima around Z = 25. This behavior would be expected if muons were in angular momentum distributions similar to those we propose for kaons. Namely, mesons in high-ℓ states rapidly reached maximum-ℓ states through transitions $\Delta n = -2, -3, \ldots$ with $\Delta \ell = -1$ and were trapped into circular orbits at n-levels where x-ray emission became dominant. Thus with the mesonic population shifted toward high-ℓ states there is less probability for $\Delta n = -2, -3, \ldots.$ transitions at low n and $(I_\beta + I_\gamma + \ldots)/I_\alpha$ is minimum. On the other hand, initial muon distributions weighted toward lower-ℓ states will proceed to low n levels in cascades more heavily weighted with $\Delta n = -2, -3, -4 \ldots$ because these higher energy transitions are favored over $\Delta n = -1$. Thus $(I_\beta + I_\gamma)/I_\alpha$ was higher for Z = 25 than for Z = 19.

These ideas are consistent with kaonic x-ray intensities where we observed higher intensities for assumed high-ℓ distributions than for low-ℓ distributions from which kaons were absorbed by nuclei instead of emitting x rays.

In Ref. 1 the x-ray intensities of O from an H_2O target appear to be abnormally low compared to neighboring elements C and Mg. In our most recent experiment we observed another instance of reduced x-ray intensity in a hydride. The intensities of a graphite target amounted to about 0.5 x rays per stopped kaon whereas a target of scintillator material, polyvinyl toluene, (CH), yielded about 0.1 x ray per kaon.

Only a small fraction of negative kaons are captured by hydrogen in a hydrocarbon. This was demonstrated by Murphy et al.[10] who found that 3.2 % of the K^- stopped in a liquid propane (C_3H_8) bubble chamber interacted with free protons. Because only a few percent of the stopped kaons were captured by hydrogen, we tentatively conclude that the hydrogen bonds in H_2O and CH had a rather enormous influence on the cascade process in C and O. In a review article, Ponomarev[11] discussed the effect of chemical bonding on pions stopped in hydrocarbons.

Another consequence of the Z-dependence of meson distributions in atomic states involves the polarization of muons in muonic atoms. Retention of the polarization of stopped muons from the instant of atomic capture depends upon the cascade mechanism.[12] Deexcitation through orbital states of maximum angular momentum preserves the original polarization more efficiently than do cascades through lower ℓ states.

It is interesting to note that Arl't et al.[13] reported that the muon polarization in graphite was 0.2 but in paraffin the polarization was 0.1. Perhaps the distribution of ℓ states due to chemical bonding contributed to the difference in polarization. Measurements of the polarization in As or Ge versus that in Cr or Mn would be instructive.

Leon and Seki[14] made a theoretical study of the atomic capture of negative mesons in which they reproduce fairly well the average values of kaonic x-ray intensities. However, their results do not show the large excursions in intensity versus Z because their model didn't take into account the individual character of atomic structure.

Fano and Dehmer[15] applied the phase-amplitude method in atomic physics to the Z-dependence of spin-orbit coupling. Fano suggested that this method should be appropriate for kaonic atoms. These calculations have not yet been made.

We summarize some implications that bear on the understanding of mesonic atoms if our ideas on initial ℓ distributions at $n = (m_K/m_e)^{\frac{1}{2}}$ are correct. (i) Chemical bonds probably influence the angular momentum distributions and thus affect x-ray emission as was indicated in certain hydrides. (ii) In muonic atoms, observed ratios of I_β/I_α versus Z are consistent with our assumptions. (iii) Polarization of muons as observed in the ground state of muonic atoms may depend on Z due to initial ℓ distributions.

An apparent enhancement of a line in the kaonic x-ray spectrum of ^{55}Mn has been resolved. We found that the intensity of the 125.95-keV line depended linearly on target thickness. The lowest nuclear state of Mn was excited by products of kaon-nucleus reactions. This was to be expected after Riddle et al.[16] found that the same line in pionic Mn was due to secondary particles. The line had appeared to be greatly enhanced because Mn was found to be at a minimum on the kaonic x-ray intensity-versus-Z curve.

A list of all the kaonic x-ray lines measured in this experiment is presented in Table II. Σ^--hyperonic lines are in Table III.

It is a pleasure to express our appreciation to Dick Pehl, Fred Goulding, Don Landis, Norman Madden, and William Hansen for furnishing us with the latest models of their superb Ge detector systems; to Billy Abram for preparing several targets of noxious elements; and to the Bevatron operators for supplying the beam.

FOOTNOTE AND REFERENCES

* Work supported by the U. S. Atomic Energy Commission.

1. Clyde E. Wiegand and Gary L. Godfrey, Phys. Rev. A 9, 2282 (1974).
2. Y. Eisenberg and D. Kessler, Phys. Rev. 130, 2352 (1963).
3. G. T. Condo, Phys. Rev. Lett. 33, 126 (1974).
4. Richard. A. Ferrell, Phys. Rev. Lett. 4, 425 (1960).
5. Z. Fried and A. D. Martin, Nuovo Cimento 29, 574 (1963).
6. J. H. Koch and M. M. Sternheim, Phys. Rev. Lett. 28, 1061 (1972); J. H. Koch, Ph. D. thesis, University of Massachusetts, 1972 (unpublished).
7. J. G. Fetkovitch *et al*. Phys. Rev. D 2, 1803 (1970).
8. G. T. Condo, Phys. Lett. 9, 65 (1964); J. E. Russell, Phys. Rev. A 1, 742 (1970).
9. D. Quitman *et al*. Nucl. Phys. 51, 609 (1964).
10. C. T. Murphy *et al*. Phys. Rev. D 9, 1248 (1974).
11. L. I. Ponomarev, Ann. Rev. Nucl. Sci. 23, 395 (1973).
12. R. A. Mann and H. E. Rose, Phys. Rev. 121, 293 (1961); V. S. Evseev, *Proceedings of the Fifth International Conference on High Energy Physics and Nuclear Structure*, Uppsala, June 1973 (to be published).
13. R. Arl't *et al*. *Proceedings of the Fifth International Conference on High Energy Physics and Nuclear Structure*, Uppsala, June 1973 (to be published).

14. M. Leon and R. Seki, Phys. Rev. Lett. 32, 133 (1974).

15. J. L. Dehmer and U. Fano, Phys. Rev. A 2, 304 (1970); J. L. Dehmer, Phys. Rev. A 7, 4 (1973); and U. Fano, private communication.

16. R. A. J. Riddle *et al*. *Proceedings of the Fifth Intenational Conference on High Energy Physics and Nuclear Structure*, Uppsala, June 1973 (to be published).

17. Ryoichi Seki, Phys. Rev. C 5, 1196 (1972).

18. G. Backenstoss, J. Egger, H. Koch, H. P. Povel, A. Schwitter, and L. Tauscher, Nucl. Phys. B73, 189 (1974).

TABLE I. Measured and calculated intensities. Intensities are absolute: e.g., for each kaon started at n = 30 in ^{32}S an average of 0.37 x rays was predicted for n = 5 → 4. Seki's exact solutions (Ref. 17) for nuclear absorption rates from n = 4, ℓ = 3 levels are higher than the perturbation values and will thus improve agreement with our experimental 4 → 3 intensities in P, S, and Cl. We point out that our ratios I(4 → 3)/I(5 → 4) are not in agreement with those of CERN (Ref. 18). Also our cascade predicts more intense $\Delta n = -2$ transitions than we find in the spectra. (The C cascade was started at n = 20.)

Z	ℓ_{max}	Transition n_i	n_f	X rays/K_{stop} measured	cal'd
6	19	4	3	0.36 ± 0.06	0.29
		3	2	0.028 ± 0.008	0.027
15	29	5	4	0.34 ± 0.06	0.37
		4	3	0.077 ± 0.015	0.11
16	29	7	6	0.24 ± 0.04	0.21
		6	5	0.36 ± 0.06	0.31
		5	4	0.36 ± 0.06	0.37
		4	3	0.047 ± 0.008	0.086
17	29	7	6	0.26 ± 0.05	0.24
		6	5	0.29 ± 0.04	0.34
		5	4	0.36 ± 0.06	0.41
		4	3	0.039 ± 0.007	0.061
25	18	7	6	0.06 ± 0.03	0.064
		6	5	0.10 ± 0.02	0.092
		5	4	0.064 ± 0.014	0.11
82	22	15	14	0.13 ± 0.05	0.12
		13	12	0.17 ± 0.05	0.15
		12	11	0.24 ± 0.04	0.21
		11	10	0.29 ± 0.05	0.27
		10	9	0.32 ± 0.05	0.32
		9	8	0.31 ± 0.05	0.36
		8	7	0.27 ± 0.05	0.35

TABLE II. Measured intensities of observed kaonic x-ray lines. Column 1 lists the targets used in the experiment. Atomic weights are shown as superscripts for targets that were practically pure isotopes. In chemical compounds, x rays listed are those of the element underlined. Column 2 contains principal quantum numbers of the initial and final states. Asterisks that precede n = 6 → 5 transitions indicate that intensities of n = 6 → 8 transitions are included because the energies are almost equal. In Column 3 are listed the electromagnetic transition energies. $M_k \equiv 493.84$ MeV. Intensities in x rays per kaon stopped in the target are listed in Column 4. Column 5 contains errors, ΔI/I, due mainly to uncertainties in the numbers of x rays in the spectral lines and should be used to compare intensities in the same element. In Column 6 are listed estimated errors in absolute intensity.

Target $^A Z$	Transition n_i	n_f	Calc'd trans. energy keV	I $\frac{\text{x rays}}{K_{stop}}$	± ΔI/I Use for error in rel. I	± ΔI Use for error in abs. I
^{12}<u>C</u>H	4	3	22.112	0.088	0.10	0.016
	5	3	32.328	0.027	0.21	0.007
	6	3	37.874	0.015	0.32	0.006
	3	2	63.321	0.017	0.51	0.009
^{14}N	5	4	14.001	0.13	0.25	0.04
	6	4	21.596	0.040	0.39	0.017
	4	3	30.294	0.38	0.05	0.06
	5	3	44.288	0.034	0.23	0.010
	6	3	51.886	0.021	0.28	0.007
	3	2	86.749	0.025	0.34	0.009
^{23}Na	7	5	30.528	0.025	0.35	0.010
	*6	5	19.054	0.26	0.14	0.05
	5	4	35.120	0.38	0.04	0.06
	6	4	54.163	0.043	0.13	0.009
	4	3	76.014	0.30	0.03	0.05
	5	3	111.110	0.028	0.25	0.008

^{27}Al	*6	5	26.715	0.23	0.11	0.04
	7	5	42.800	0.053	0.34	0.019
	5	4	49.244	0.34	0.05	0.05
	6	4	75.942	0.036	0.23	0.010
	7	4	92.032	0.033	0.32	0.012
	4	3	106.598	0.18	0.08	0.03
^{40}Ar	7	6	31.077	0.42	0.14	0.09
	*6	5	51.596	0.48	0.06	0.08
	7	5	82.650	0.044	0.14	0.009
	5	4	95.126	0.49	0.04	0.08
	6	4	146.697	0.050	0.15	0.011
	4	3	205.972	0.056	0.41	0.024
K	9	7	37.827	0.038	0.28	0.012
	10	7	48.823	0.023	0.24	0.007
	7	6	34.622	0.15	0.11	0.03
	9	6	72.439	0.015	0.23	0.004
	*6	5	57.483	0.28	0.03	0.04
	7	5	92.079	0.038	0.10	0.007
	8	5	114.525	0.013	0.24	0.004
	5	4	105.985	0.27	0.03	0.04
	6	4	163.418	0.022	0.20	0.006
Ca	7	6	38.381	0.19	0.24	0.06
	*6	5	63.727	0.32	0.07	0.05
	7	5	102.078	0.042	0.40	0.018
	5	4	117.502	0.33	0.08	0.06
^{55}Mn (2.0)	8	7	39.056	0.094	0.55	0.054
	7	6	60.232	0.028	0.55	0.016
	*6	5	100.021	0.074	0.19	0.018
	5	4	184.465	0.11	0.39	0.04
	^{a}Mn*		(125.95)	0.076	0.24	0.022

^{55}Mn (5.2)	7	6	60.232	0.064	0.45	0.030
	*6	5	100.021	0.12	0.09	0.02
	^{b}7	5	160.196	0.062	0.38	0.026
	5	4	184.465	0.066	0.16	0.015
	^{c}Mn*		(125.95)	0.23	0.05	0.04
Fe	8	7	42.255	0.10	0.58	0.06
	7	6	65.168	0.074	0.30	0.025
	*6	5	108.220	0.11	0.21	0.03
^{75}As	9	8	46.783	0.24	0.33	0.09
	8	7	68.296	0.31	0.13	0.06
	9	7	115.034	0.042	0.49	0.021
	7	6	105.345	0.33	0.10	0.06
	*6	5	174.977	0.49	0.13	0.10
Se	10	8	85.168	0.12	0.48	0.06
	8	7	72.533	0.39	0.22	0.10
	7	6	111.883	0.56	0.13	0.11
	*6	5	185.843	0.44	0.31	0.15
Rb	10	9	42.091	0.46	0.32	0.16
	11	9	73.189	0.11	0.42	0.05
	9	8	58.888	0.24	0.26	0.07
	10	8	100.940	0.11	0.45	0.05
	8	7	85.974	0.45	0.10	0.08
	9	7	144.800	0.13	0.41	0.06
	7	6	132.625	0.42	0.08	0.07
	*6	5	220.319	0.37	0.14	0.07
Sr	9	8	62.131	0.19	0.47	0.09
	8	7	90.709	0.31	0.17	0.07
	7	6	139.932	0.42	0.13	0.08
	*6	5	232.467	0.28	0.32	0.10

^{89}Y	9	8	65.457	0.23	0.23	0.06
	10	8	112.195	0.046	0.41	0.020
	8	7	95.566	0.27	0.10	0.05
	9	7	160.949	0.044	0.42	0.020
	7	6	147.428	0.30	0.09	0.05
	*6	5	244.929	0.25	0.18	0.06
Zr	10	9	49.227	0.32	0.46	0.16
	9	8	68.874	0.33	0.19	0.08
	8	7	100.558	0.39	0.12	0.07
	7	6	155.132	0.29	0.18	0.07
^{93}Nb	9	8	72.376	0.19	0.33	0.07
	10	8	124.051	0.085	0.49	0.043
	8	7	105.672	0.29	0.14	0.06
	7	6	163.027	0.32	0.12	0.06
	*6	5	270.864	0.37	0.24	0.10
Mo	10	9	54.298	0.10	0.85	0.09
	9	8	75.972	0.23	0.25	0.07
	10	8	130.211	0.078	0.42	0.035
	8	7	110.924	0.31	0.17	0.07
	7	6	171.132	0.31	0.20	0.08
Pd	9	8	91.221	0.22	0.45	0.10
	8	7	133.198	0.26	0.23	0.07
	7	6	205.517	0.38	0.43	0.17
Sn	10	9	77.092	0.17	0.49	0.09
	9	8	107.875	0.16	0.42	0.07
	8	7	157.527	0.21	0.36	0.08
Sb	9	8	112.258	0.36	0.23	0.10
	8	7	163.930	0.24	0.35	0.09
	7	6	252.969	0.42	0.28	0.13

Te	10	9	83.424	0.27	0.24	0.08
	9	8	116.738	0.29	0.14	0.06
	8	7	170.476	0.32	0.11	0.06
	7	6	263.079	0.22	0.23	0.06
Ba	11	10	71.576	0.25	0.35	0.10
	10	9	96.817	0.24	0.17	0.05
	9	8	135.487	0.23	0.12	0.04
	8	7	197.870	0.30	0.10	0.05
	7	6	305.390	0.26	0.15	0.06
^{139}La	12	11	56.370	0.33	0.49	0.17
	11	10	74.164	0.24	0.30	0.08
	10	9	100.319	0.22	0.18	0.05
	9	8	140.390	0.26	0.12	0.05
	8	7	205.035	0.26	0.12	0.05
	7	6	316.457	0.26	0.18	0.06
Ce	11	10	76.798	0.56	0.49	0.28
	10	9	103.883	0.34	0.30	0.11
	9	8	145.379	0.24	0.26	0.07
	8	7	212.326	0.32	0.23	0.09
Nd	12	10	144.611	0.065	0.35	0.025
	11	10	82.208	0.20	0.38	0.08
	10	9	111.203	0.25	0.11	0.05
	9	8	155.629	0.23	0.09	0.04
	8	7	227.305	0.25	0.10	0.05
	7	6	350.863	0.22	0.16	0.05
Sm	12	11	66.737	0.64	0.43	0.29
	11	10	87.808	0.46	0.32	0.16
	10	9	118.780	0.28	0.29	0.09
	9	8	166.237	0.25	0.29	0.08
	8	7	242.810	0.38	0.25	0.11

Gd	10	9	126.610	0.33	0.24	0.09
	9	8	177.201	0.30	0.22	0.08
	8	7	258.836	0.35	0.27	0.11
Dy	11	10	99.562	0.081	0.34	0.030
	10	9	134.687	0.16	0.17	0.04
	11	9	234.086	0.052	0.38	0.021
	9	8	188.511	0.19	0.12	0.04
	8	7	275.368	0.19	0.13	0.04
^{165}Ho	11	10	102.615	0.091	0.41	0.040
	12	10	180.488	0.054	0.42	0.024
	10	9	138.819	0.25	0.12	0.05
	9	8	194.297	0.17	0.15	0.04
	8	7	283.827	0.21	0.16	0.05
Er	11	10	105.715	0.18	0.21	0.05
	10	9	143.013	0.23	0.13	0.05
	11	9	248.549	0.043	0.46	0.021
	9	8	200.172	0.19	0.14	0.04
	8	7	292.415	0.18	0.15	0.04
Yb	11	10	112.055	0.22	0.39	0.09
	10	9	151.594	0.24	0.29	0.08
	9	8	212.189	0.19	0.33	0.07
	8	7	309.985	0.36	0.26	0.11
Hf	10	9	160.426	0.32	0.26	0.10
	9	8	224.559	0.18	0.36	0.07
Pt	12	11	105.837	0.27	0.35	0.10
	11	10	139.273	0.26	0.22	0.07
	10	9	188.435	0.23	0.19	0.06
	11	9	327.422	0.089	0.49	0.046
	9	8	263.792	0.23	0.18	0.05
	8	7	385.449	0.19	0.34	0.07

Hg	11	10	146.542	0.12	0.40	0.05
	10	9	198.275	0.15	0.26	0.05
	9	8	277.578	0.16	0.32	0.06

*) Intensities are sums of $n = 6 \rightarrow 5$ and $n = 8 \rightarrow 6$.

a) Nuclear γ ray of excited ^{55}Mn. Target thickness 2.0 g cm^{-2}.

b) Mn $n = 7 \rightarrow 5$ possibly includes ^{47}Ti nuclear γ ray.

c) Nuclear γ ray of excited ^{55}Mn. Target thickness 5.2 g cm^{-2}.

TABLE III. Intensities of Σ^--hyperonic x-ray lines. Calculated energies do not include vacuum polarization or corrections for finite nuclear size. Intensities are in x rays per stopped kaon.

Target ^{A}Z	Tran-sition n_i	n_f	Calc'd trans. energy keV	I $\frac{\text{x rays}}{K_{stop}}$	$\pm\Delta I/I$ Use for error in rel. I	$\pm\Delta I$ Use for error in abs. I
^{14}N	5	4	32.4	0.021	0.35	0.008
^{23}Na	[a]7	6	25.6	0.019	0.69	0.013
	6	5	44.1	0.019	0.39	0.008
	5	4	83.1	0.016	0.23	0.004
^{27}Al	6	5	63.1	0.021	0.36	0.008
^{40}Ar	[a]7	6	74.1	0.034	0.26	0.010
	6	5	122.4	0.029	0.26	0.009
K	8	7	53.3	0.015	0.37	0.006
	[a]7	6	82.8	0.015	0.47	0.007
	6	5	137.1	0.007	0.47	0.003

a) Includes K, $n = 10 \rightarrow 6$ which is estimated to contribute about $0.02\, I_{max}$ where I_{max} is the most intense kaonic line of the target.

FIGURE CAPTION

Fig. 1. Intensity versus Z of observed principal ($\Delta n = -1$) kaonic x-ray lines. Error bars include statistical uncertainties in the numbers of recorded x rays, but do not include errors in the absolute numbers of stopped kaons which we estimate to be $\pm$ 15%. Filled-in circles apply to data of Ref. 1; open squares to our recent experiment.

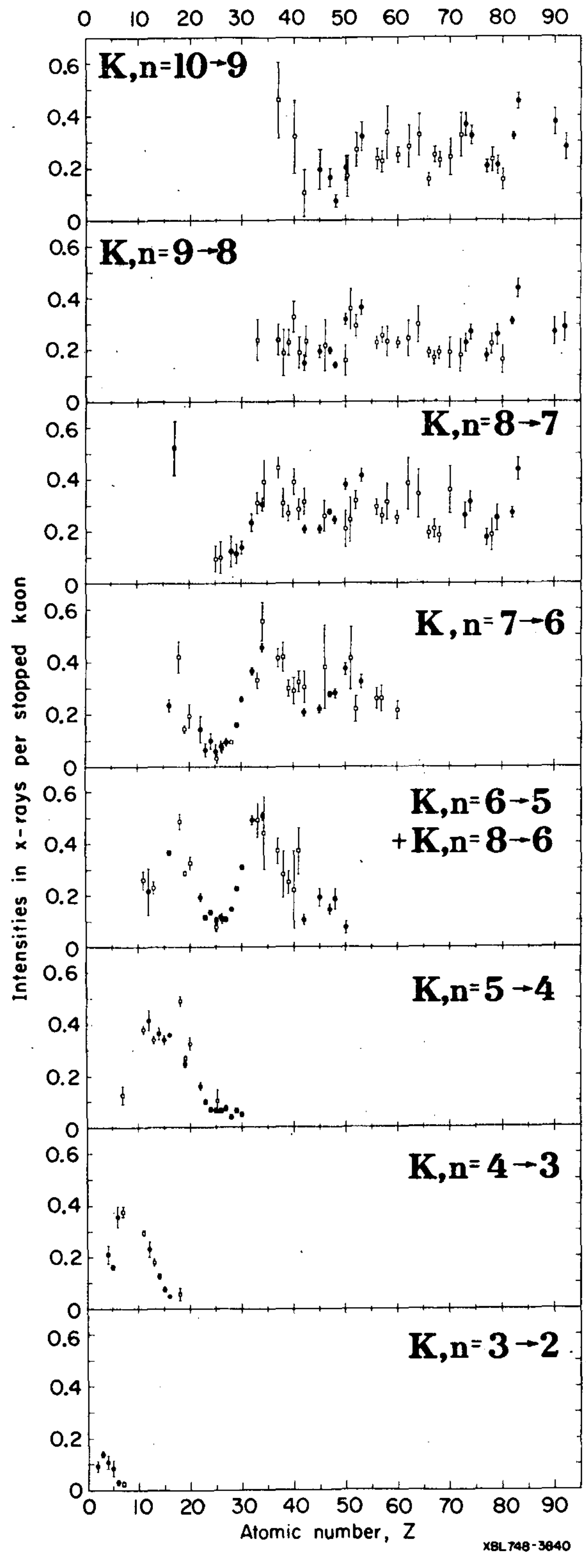

K,n=10→9
K,n=9→8
K,n=8→7
K,n=7→6
K,n=6→5
+K,n=8→6
K,n=5→4
K,n=4→3
K,n=3→2
Intensities in x-rays per stopped kaon
Atomic number, Z
XBL 748-3840

Fig. 1.

0 0 0 0 4 1 0 7 9 2 7

TECHNICAL INFORMATION DIVISION
LAWRENCE BERKELEY LABORATORY
UNIVERSITY OF CALIFORNIA
BERKELEY, CALIFORNIA 94720